Load Frequency Control of an Autonomous Microgrid Using Robust Fuzzy PI Controller

Anil Annamraju, Srikanth Nandiraju
Department of Electrical Engineering
NIT Warangal
Warangal, India
ani223kumar@gmail.com, nvs@nitw.ac.in

***Abstract*— This paper proposes a robust load frequency control (LFC) strategy using fuzzy logic based PI controller for an autonomous hybrid microgrid with high renewable penetration. Such a high amount of renewable energy sources (RES) penetration replaces the contribution of diesel engine generators (DEGs), which intern reduces the system inertia as a result; microgrid (MG) experiences a frequency instability problem. Furthermore, the intermittent nature of the RES, load shedding and load restoring causes large frequency deviations which may weaken the MG and could lead to complete blackout. To solve the aforementioned problem, this work proposes an optimal coordinated control strategy between DEGs and SMES system for MG frequency control. Where this coordinated control strategy is based on the PI controller, which is optimally tuned by using a fuzzy logic approach. This proposed control strategy is tested on the BELLA-COOLA MG (in Canada), which was modelled in MATLAB/ Simulink. Finally, the simulation outcomes confirm the robustness and effectiveness of the proposed approach against all possible critical operational scenarios over various controllers in literature.**

Keywords—Microgrid, robust controller, frequency control, SMES, fuzzy logic approach based PI controller.

I. INTRODUCTION

The increasing energy demand from distant places like rural areas and islands from the main grid is very costly, environmentally hazardous and complicated in the present power system scenario. For such conditions, an autonomous MG would be an efficient and reliable solution. The MG comprises various RES which are intermittent by nature and this intermittency of RES brings new operational challenges for grid stability, particularly in frequency deviation control [1].

Frequency deviation in the power system is a direct consequence of the mismatch between the load demand and the power generation. A long-term system frequency deviation from the rated value (50Hz or 60 Hz) is harmful to the secure operation of the power system/MG. LFC is of the utmost importance in such a scenario. It operates constantly to maintain a balance between the load demand and the power generation and tries to restore the grid frequency to the rated value [2].

In a traditional power system, the LFC task is quite simple since the disturbances arise from the load side only. Whereas in MG, the LFC task is complex due to the intermittent nature of RES, the stochastic nature of the load and low system inertia. The above factors create large frequency deviations in MG which may lead to the system blackout. So, to ensure the frequency stability in an autonomous MGs, energy storage systems (ESSs) have turned into a vital part. Among all ESSs, SMES form the best option for LFC studies due to its instantaneous reaction to frequency changes. Moreover, unlike other ESSs, SMES does not have any moving parts and less power wastage [3].

During the last decade, several authors proposed various LFC strategies by incorporating ESSs in MG [4-13]. In [4] authors proposed a fixed gain PI/ PID controller, in [5] an adaptive droop control method, in [6] with the model predictive controller, in [7] with the internal model-based controller, in [8] with an H_∞ based controller, etc. In [9-13] the authors proposed various meta-heuristic approaches for MG frequency control. In [9] with genetic algorithm optimized PID controller, in [10] with the PSO (particle swarm optimization) algorithm, in [11] with the harmony search algorithm, in [12] with the social-spider optimization algorithm, in [13] with the grasshopper optimization algorithm, etc.

The above controllers proposed in the literature [6, 8, 9-13] suffer from the drawback of being complex in nature, and may not provide optimal performance by virtue of inappropriate selection of their algorithm-specific parameters. The improper selection of these parameters increases the computational complexity of the algorithm. Moreover, these controllers can perform optimally only when a definite mathematical model of the system is available.

From the literature, the fuzzy logic approach (FLA) is proven as an efficient solution where the precise mathematical model is not available. Few studies are reported on the LFC design of MG with FLA based gain scheduling of PI controller [14, 15]. The technical problem with this type of approach is the structure of the PI controller would be changed when the specifications of the system change, which affects the steady-state response of the system. To conquer the above problem, this work comes up with a new approach by maintaining the structure of the PI controller as it is and by extending its robustness through a fuzzy logic approach based corrective loop in accordance with disturbances.

978-1-7281-4103-9/19/$31.00©2019IEEE

II. MICROGRID MODELLING

Fig.1 illustrates a linearized model of BELLA-COOLA MG. This model consists of SMES, DEG, RES like wind turbine generator (WTG) and PV, load model along with a battery energy system. In detail explanation regards to each MG component is explained in the subsections. The simulation parameters of MG are listed in Table I.

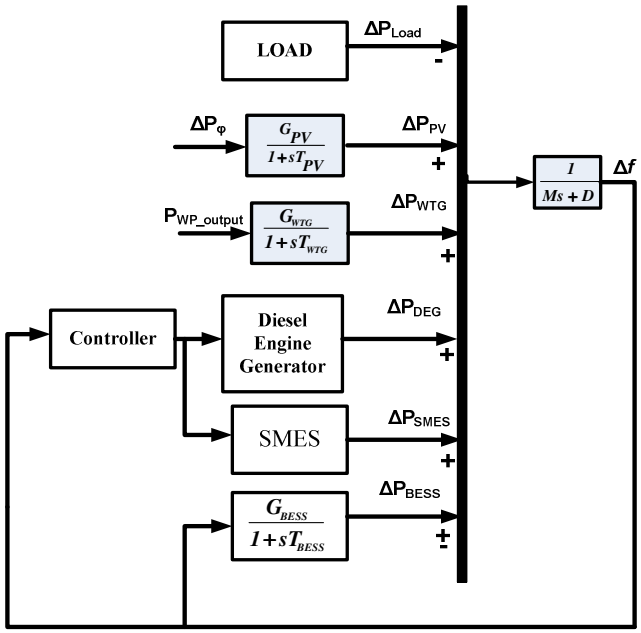

Fig.1 Block diagram of BELLA-COOLA MG

From Fig.1, the MG output power balance equation can be written as:

$$\Delta P_{LOAD} = \Delta P_{WTG} + \Delta P_{PV} \pm \Delta P_{BESS} + \Delta P_{DEG} + \Delta P_{SMES} \quad (1)$$

Where ΔP_{LOAD} indicates a change in load; ΔP_{WTG} indicates a change in the WTG power output; ΔP_{PV} indicates a change in the PV power output; ΔP_{DEG} indicates a change in the DEG power output; ΔP_{SMES} indicates a change in the SMES power output; ΔP_{BESS} indicated change in a battery power output. '±' sign indicates opposite action from the battery storage system with respect to Δf of MG since it resides in primary frequency control. The residual power in MG (ΔP_e) load-generation imbalance can be expressed as:

$$\Delta P_e = \Delta P_{MG} - \Delta P_{Load} \quad (2)$$

Where ΔP_{MG} indicates change in the MG power constituted by all sources in response to load changes (ΔP_{LOAD}). Due to the volatile nature of RES, these RES are not considered in LFC. Only DEG and SMES are responsible for generation-load balance (i.e. $\Delta P_e = 0$) with the assistance of FLA based PI controller.

A. DEG Modeling

In remote villages and islands, demand is increasing, but due to financial and technical constraints, high voltage grid line extension is prohibiting. Therefore constant speed diesel generators are used which consists of a diesel engine generator and governor. Fig.2 illustrates the mathematical modelling of DEG [15]. Where ΔX indicates a change in valve position according to the control signal (U_c).

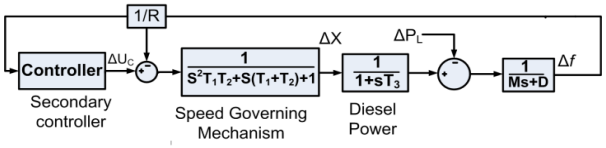

Fig.2 Mathematical model of DEG

B. PV model

In PV array, the combination of modules in series and parallel and this combination relies on the desired voltage and current ratings of the MG. The output power of the PV array (P_{PV}) can be expressed as:

$$P_{PV} = \frac{\varphi}{\varphi_{stc}} S[1\text{-}0.005(T_a + 25)] \quad (3)$$

Where φ_{stc} indicates the irradiation at standard reference temperature; φ indicates the irradiation at actual condition; S indicates the measured area of PV array. The first-order model of the PV system can be expressed as:

$$TF_{PV} = \frac{\Delta P_{PV}}{\Delta \varphi} = \frac{G_{PV}}{1+sT_{PV}} \quad (4)$$

Where $\Delta\varphi$ indicates a change in the irradiation; G_{PV} indicates the gain of the PV array; T_{PV} indicates the time constant of PV array including converter time delay also.

Table I Simulation parameters of MG

Parameter	Value	Parameter	Value
M(s)	0.1667	T_2(s)	2
D(puMW)	0.015	T_3(s)	3
G_{BESS}	1.5	T_{BESS}(s)	0.1
G_{WTG}	1	T_{SMES}(s)	0.01
G_{PV}	1	T_{PV}(s)[Including converter time constant]	1.5
T_1(s)	0.025	T_{WTG}(s) [Including converter time constant]	2

C. WTG model

Fig.3 depicts a mathematical model for a random wind power generation. In this model, the random speed (which obtains from white noise block) is multiplied with constant wind speed ($P_{WP\_initial}$) and then with some arithmetic operations, the required WTG output power fluctuation (P_{WP_output}) response curve is obtained.The transfer function model of the WTG system can be expressed as:

$$TF_{PV} = \frac{\Delta P_{WTG}}{P_{WP\_output}} = \frac{G_{WFG}}{1+sT_{WTG}} \quad (5)$$

Where G_{WTG} indicates the gain of the WTG system; T_{WTG} indicates the time constant of WTG array with including converter time delay also.

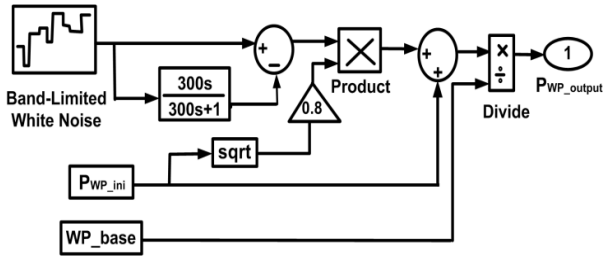

Fig.3 Mathematic model for a random wind power generation

D. SMES model

Fig.4 illustrates the mathematical modeling of SMES. The output power of SMES for discharging or charging is chosen based on the reference signal (U_c) from the controller. In the present work, the U_c is determined by using the FLA based PI controller.

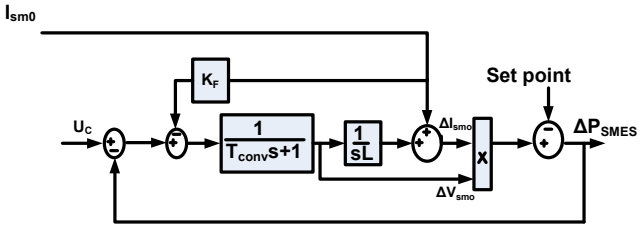

L: Inductance of super conduction coil (2.5 H); T_{conv}: Convertor time constant(0.03 s), I_{sm0}: Nominal DC current (1 KA)

Fig.4 The Mathematical model of SMES for LFC

Where I_{sm} denotes the initial value of DC current flowing through SMES coil; ΔV_{sm} indicates the change in SMES voltage; ΔI_{sm} indicates the change in SMES current.

Based on the control signal received from the controller ($U_c(s)$), the input signal of the SMES control loop controls the $\Delta V_{sm}(s)$ continuously. With respect to this, immediate action to the next load change needs to the fast restoration of I_{sm0} to its nominal value. To perform this task, ΔI_{sm} is assigned with negative feedback in the control loop. Correspondingly, the voltage across the inductor from the converter (ΔV_{sm}) and inductor current deviations (ΔI_{sm}) can bewritten as follows:

$$\Delta V_{sm}(s) = \frac{1}{1+sT_{conv}} U_c(s) - \frac{K_F}{1+sT_{conv}} \Delta I_{sm}(s) \quad \& \quad \Delta I_{sm}(s) = \frac{1}{sL} \Delta V_{sm}(s)$$

Finally, ΔP_{SMES} based on the reference signal is expressed as:

$$\Delta P_{SMES} = \Delta V_{sm} * (I_{sm} + \Delta I_{sm}) \tag{6}$$

III. FLA BASED PI CONTROLLER

The typical PI controllers like Zieger-Nicholas tuned PI controller associated with fixed gains which are determined based on predetermined operating conditions of the system.

Due to rapid changes in the operating conditions of MG, Z-N tuned PI controller doesn't guarantee optimal performance in a situation of rapid change in operating conditions. Assuming that, the rapid changes in MG can be traced by PI controller, the optimal performance will be achieved. To perform this task FLA is employed in this work.

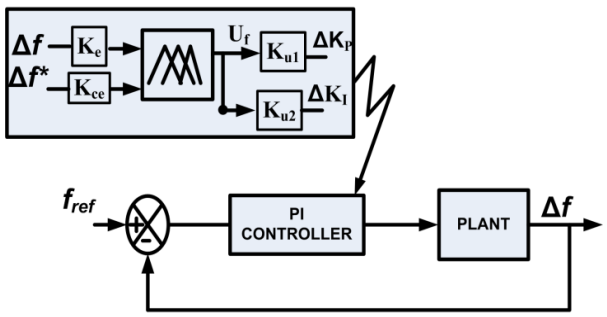

(a)

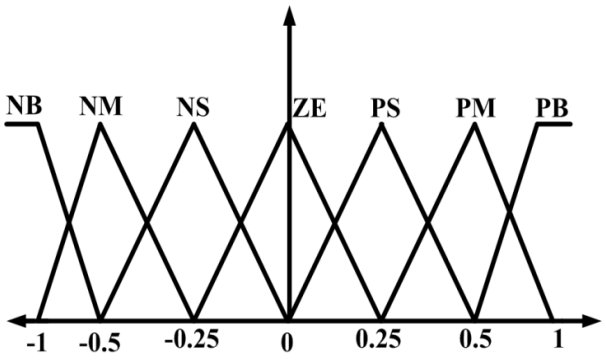

(b)

Fig.5 (a) Structure of the FLA-PI controller, (b) MFs of inputs and output of FLA-PI

Fig.5(a) depicts the structure of the proposed FLA based PI controller. FLA is employed due to its effectiveness in handling the uncertainties of the various systems in literature [15]. In Fig.5, frequency deviation(Δf) and change in frequency deviations (Δf*) are inputs of FLA and updating factor (U_f) is the output of FLA. The change in the gains of the PI controller (ΔK_P & ΔK_I) based on FLA output can be expressed as:

$$\begin{aligned} \Delta K_P &= U_f * K_{S1} \\ \Delta K_I &= U_f * K_{S2} \end{aligned} \tag{7}$$

Where, K_{S1} & K_{S2} are the scaling factors of the FLA output. Finally, the FLA tuned PI controller can be expressed as:

$$U_c = (K_P + U_f * K_{S1}) + \frac{(K_I + U_f * K_{S2})}{s} \tag{8}$$

Where U_c is the command signal generated by the FLA-PI controller to DEG and SMES.

The FLC is formulated using MFs for the input parameters such as Δf & Δf*, which are defined as:

$$\begin{aligned} \Delta f &= f_{ref} - f \\ \Delta f^* &= \Delta f(k-1) - \Delta f(k) \end{aligned} \tag{9}$$

The MFs for the inputs and output of FLC are shown in Fig.5 (b). Two inputs with seven fuzzy sets (7^2), FLA consists of 49 rules to resemble different operating conditions as mentioned in Table II. In the proposed approach, to create the maximum degree of freedom in the tuning process of PI controller, 49 rules are employed. As per human information processing capability limit, the number of fuzzy sets per variable should not be higher than 7.

The output of FLA (U_f) from fuzzy reasoning is calculated by using Eq. (10):

$$U_f = \frac{\sum_{i=1}^{49} \mu_i w_i}{\sum_{i=1}^{49} w_i} \quad (10)$$

Where μ_i is the degree of membership of i^{th} input combination and w_i is the weight of the i^{th} rule.

Table II Fuzzy rule base

Δf	$\Delta f^{\#}$						
	NB	**NM**	**NS**	**ZE**	**PS**	**PM**	**PB**
NB	PB	PB	PB	PB	PM	PS	ZE
NM	PB	PB	PB	PM	PS	ZE	NS
NS	PB	PB	PM	PS	ZE	NS	NM
ZE	PB	PM	PS	ZE	NS	NM	NB
PS	PM	PS	ZE	NS	NM	NB	NB
PM	PS	ZE	NS	NM	NB	NB	NB
PB	ZE	NS	NB	NB	NB	NB	NB

IV. RESULTS AND DISCUSSIONS

In this section, the frequency response of MG has been analyzed with various disturbances like ΔP_{Load}, ΔP_{WTG} and ΔP_{φ} in addition to the parametric uncertainties. How better the improvement in the dynamic response of proposed controller over other controllers in literature like the PSO-PI controller and the Zieger-Nicholas tuned PI controller is demonstrated with different operating scenarios. Moreover, the effect of SMES on the MG frequency response is analyzed in the special scenario.

A. *Scenario 1*

Test condition: A step –change on load demand (ΔP_{Load}) of 0.025 p.u and 0.1 p.u. in RES ($\Delta P_{WTG} + \Delta P_{PV}$) power at an instant of 20 seconds and 120 seconds respectively. Fig.6 depicts the frequency deviation response of MG for scenario 1 with various controllers. The quantitative analysis of Fig.6 is given in the Table III.

B. *Scenario 2*

Test condition: A random wind power fluctuation (ΔP_{WTG}) alone is considered as a disturbance in MG.

Table III Quantitative analysis of scenario 1

Methods	Performance indices			
	Peak Undershoot (Hz)	Settling time (sec)	Peak overshoot(Hz)	Settling Time (Sec)
Z-N PI	49.97	20	50.107	23
PSO-PI	49.98	13	50.094	14
FLA-PI	**49.99**	**7**	**50.042**	**7**

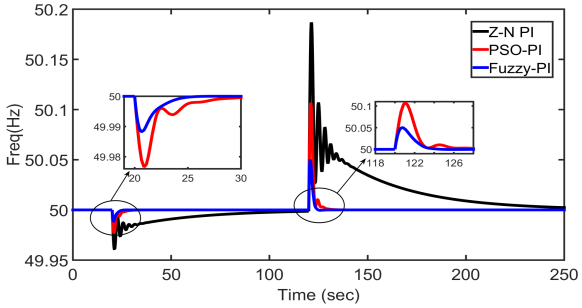

Fig.6 Frequency deviation response of MG for scenario 1

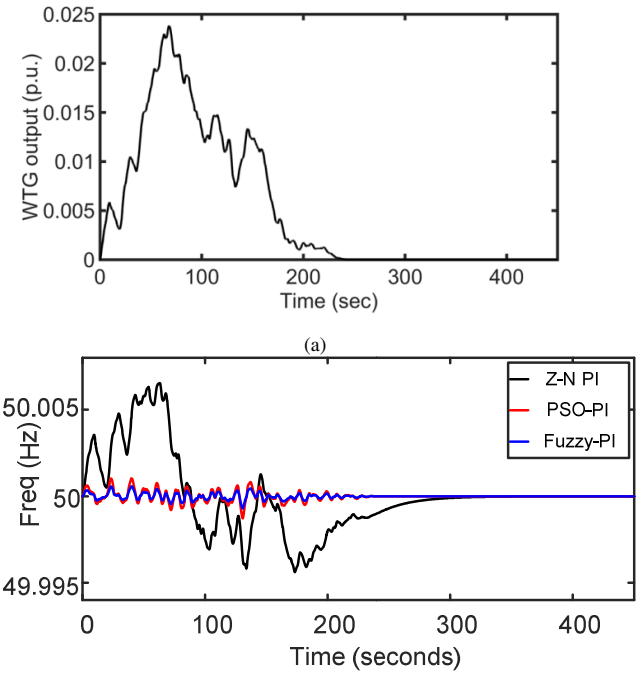

Fig.7 (a) WTG output power fluctuations (b) Frequency deviation response of MG for scenario 2

Fig.7(a) illustrates the random wind power fluctuations in MG and Fig.7(b) depicts the frequency deviation response of MG for scenario 2 with various controllers.

C. *Scenario 3*

Test condition: A multiple step PV power fluctuations (ΔP_{PV}) alone is considered as a disturbance in MG.

Fig.8(a) illustrates the multiple step PV power fluctuations in MG and Fig.8(b) depicts the frequency deviation response of MG for scenario 3 with various controllers.

D. *Scenario 4*

Test condition: ΔP_{Load} , ΔP_{WTG} and ΔP_{PV} are simultaneously applied as disturbances to MG.

Fig.9(a) illustrates the multiple disturbances applied concurrently to MG and Fig.9(b) depicts the frequency deviation response of MG for scenario 4 with various controllers.

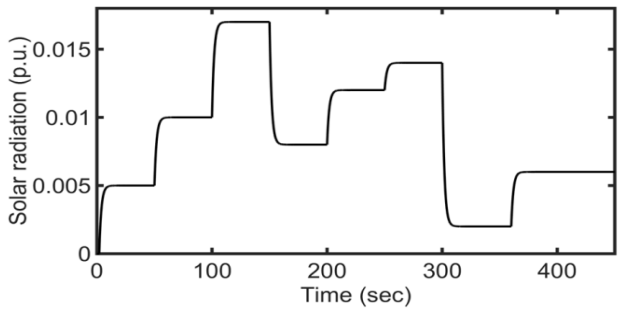

(a)

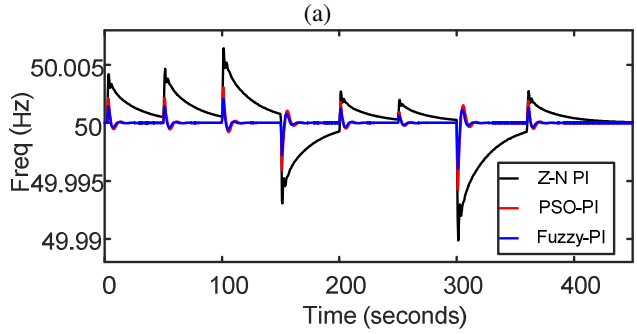

(b)

Fig.8 (a) PV power output fluctuations (b) Frequency deviation response of MG for scenario 3

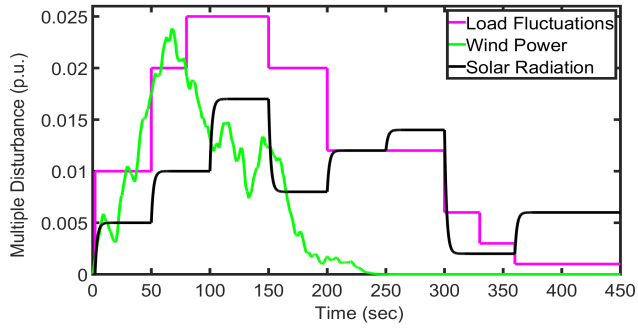

(a)

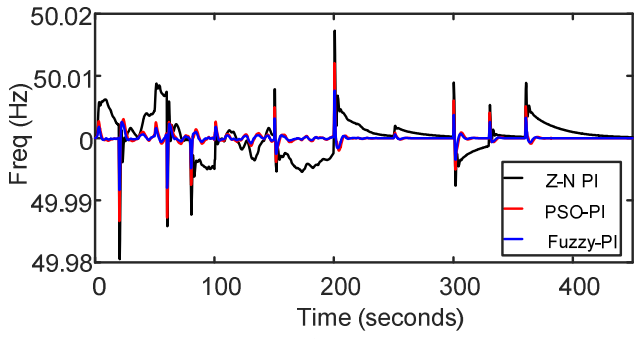

(b)

Fig.9 (a) Concurrent changes in PV power, WTG power, and Load (b) Frequency deviation response of MG for scenario 4

From the results of the simulation of scenario 4, it is evident that the conventional PI controller fails to provide acceptable performance when concurrent changes in the microgrid. However, PSO-PI and proposed Fuzzy-PI provides a stable performance. In this duo, the proposed controller provides a superior dynamic response over PSO-PI. The computational complexity of various controllers with integral time absolute error as criteria (this term is used to define total magnitude of frequency deviation over total simulation time) is given in Table IV.

Table IV Computational complexity of various controllers

Methods	Computation time based on ITAE tolerance of 0.005 (in seconds)			
	Scenario 1	Scenario 2	Scenario 3	Scenario 4
Z-N PI	53	44	39	Unstable
PSO-PI	31	27	23	72
FLA-PI	**15**	**13**	**10**	**48**

E. Scenario 5

The objective of this scenario is to demonstrate the impact of SMES in minimizing the frequency deviations of the MG. For this scenario, three control mechanisms are considered. These are:

1. Without any LFC scheme
2.With fuzzy tuned PI LFC scheme, but without any SMES
3. With the proposed fuzzy tuned PI LFC scheme coordinated with SMES

Test condition: test conditions are similar to Fig.9 (a). In addition to that 50% reduction in system inertia(H) and load damping coefficient (D), 20% increase in governor time constant (T_G) are considered as parametric uncertainties. Fig.10 depicts the frequency deviation response of MG for scenario 5.

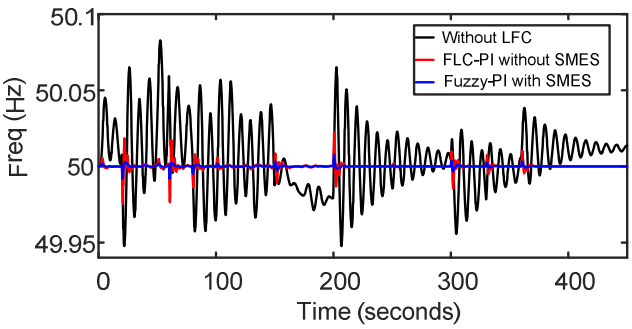

Fig.10 Frequency deviation response of MG with and without SMES

The following observations are made from the extensive LFC analysis on MG simulation with possible operating scenarios.

1. Scenario 1,2 & 3 reveals the superiority of the proposed fuzzy tuned PI controller in improving the dynamic frequency response of the system for step load, solar and wind power disturbances over other controllers in the literature.
2. Scenario 4 revealed the supremacy of the proposed fuzzy tuned PI controller against concurrent disturbances from the load side as well as from the renewable side along with

severe parametric uncertainties. It is also noticed that MG frequency deviation fails to stabilize with conventional PID. Whereas, PSO-PID had experienced large overshoots and more settling times in this scenario.

3. Scenario 5 depicts the superiority of the proposed coordinated control strategy[DEG+SMES+Fuzzy-PI] in improving the frequency response of the MG over without SMES coordination [DEG + Fuzzy -PI].

V. CONCLUSIONS

In this work, a robust fuzzy PI controller is proposed for the comprehensive LFC analysis of an autonomous MG integrated with SMES. The proposed controller simulation outcomes are compared with the PSO-PI controller and Zieger-Nicholas tuned PI controller under different operating scenarios. From the simulation outcomes of all scenarios, the proposed controller exhibits a better dynamic performance in terms of overshoot reduction, fast settling time and less frequency deviation error over other controllers in the literature. Moreover, the effect on LFC of MG due to SMES is analyzed, and it is noticed that the dynamic performance of the system is significantly improved with interaction of SMES with DEGs as compared to the case when SMES is not connected.

REFERENCES

[1] IEEE Guide for Design, Operation, and Integration of Distributed Resource Island Systems with Electric Power Systems," in *IEEE Std 1547.4-2011*, pp.1-54, 20 July 2011.

[2] D. Lee and L. Wang, "Small-Signal Stability Analysis of an Autonomous Hybrid Renewable Energy Power Generation/Energy Storage System Part I: Time-Domain Simulations," *IEEE Trans. Energy Convers.*, vol. 23, no. 1, pp. 311–320, 2008.

[3] A. Cansiz, C. Faydaci, M. T. Qureshi, O. Usta, and D. T. McGuiness, "Integration of a SMES–Battery-Based Hybrid Energy Storage System into Microgrids," *J. Supercond. Nov. Magn.*, vol. 31, no. 5, pp. 1449–1457, 2018.

[4] P. K. Ray, S. R. Mohanty, and N. Kishor, "Proportional–integral controller based small-signal analysis of hybrid distributed generation systems," *Energy Convers. Manag.*, vol. 52, no. 4, pp. 1943–1954, 2011.

[5] J. Li, R. Xiong, Q. Yang, F. Liang, M. Zhang, and W. Yuan, "Design/test of a hybrid energy storage system for primary frequency control using a dynamic droop method in an isolated microgrid power system," *Appl. Energy*, vol. 201, pp. 257–269, Sep. 2017.

[6] J. Pahasa and I. Ngamroo, "Coordinated Control of Wind Turbine Blade Pitch Angle and PHEVs Using MPCs for Load Frequency Control of Microgrid," *IEEE Syst. J.*, vol. 10, no. 1, pp. 97–105, 2016.

[7] W. Tan, "Unified Tuning of PID Load Frequency Controller for Power Systems via IMC," in *IEEE Transactions on Power Systems*, vol. 25, no. 1, pp. 341-350, 2010.

[8] H. Bevrani, M. R. Feizi and S. Ataee, "Robust Frequency Control in an Islanded Microgrid: H_∞ and μ Synthesis Approaches," in *IEEE Transactions on Smart Grid*, vol. 7, no. 2, pp. 706-717, March 2016

[9] D. C. Das, A. K. Roy, and N. Sinha, "GA based frequency controller for solar thermal–diesel–wind hybrid energy generation/energy storage system," *Int. J. Electr. Power Energy Syst.*, vol. 43, no. 1, pp. 262–279, 2012.

[10] S. K. Pandey, S. R. Mohanty, N. Kishor, and J. P. S. Catalão, "Frequency regulation in hybrid power systems using particle swarm optimization and linear matrix inequalities based robust controller design," *International Journal of Electrical Power & Energy Systems*, vol. 63, pp. 887–900, 2014.

[11] G. Shankar and V. Mukherjee, "Load frequency control of an autonomous hybrid power system by quasi-oppositional harmony search algorithm," *Int. J. Electr. Power Energy Syst.*, vol. 78, pp. 715–734, 2016.

[12] A. A. El-Fergany and M. A. El-Hameed, "Efficient frequency controllers for autonomous two-area hybrid microgrid system using social-spider optimiser," *IET Gener. Transm. Distrib.*, vol. 11, no. 3, pp. 637–648, 2017.

[13] A. Annamraju and S. Nandiraju, "Frequency Control in an Autonomous Two-area Hybrid Microgrid using Grasshopper Optimization based Robust PID Controller," *2018 8th IEEE India International Conference on Power Electronics (IICPE)*, JAIPUR, India, 2018, pp. 1-6.

[14] M. R. Sathya and M. Mohamed Thameem Ansari, "Load frequency control using Bat inspired algorithm based dual mode gain scheduling of PI controllers for interconnected power system," *International Journal of Electrical Power & Energy Systems*, vol. 64, pp. 365–374, 2015.

[15] A.Annamraju and S.Nandiraju "Robust frequency control in an autonomous microgrid: A two-stage adaptive fuzzy Approach ," *Electric Power components and systems*, Vol.46 (1), pp.83-94, 2018.